AIAA 97-1854
Transonic Wing Optimization Using Genetic Algorithm

A. Oyama, S. Obayashi, and K. Nakahashi,
Tohoku Univ., Sendai, Japan;
T. Nakamura,
National Aerospace Lab, Tokyo, Japan

Transonic Wing Optimization Using Genetic Algorithm

A. Oyama, S. Obayashi, K. Nakahashi

Tohoku University, Sendai, Japan

and

T. Nakamura

National Aerospace Laboratory, Tokyo, Japan

Abstract[1]

A Genetic Algorithm (GA) has been applied to optimize a transonic wing shape for generic transport aircraft. A three-dimensional compressible Navier-Stokes (N-S) solver is used to evaluate aerodynamic performance. The N-S evaluation is parallelized on Numerical Wind Tunnel (NWT) at National Aerospace Laboratory in Japan, a parallel vector machine with 166 processing elements. Designed wings show a tradeoff between an increase of the airfoil thickness driven by a structural constraint and a reduction of the wave drag produced by a shock wave. The present result indicates that GA has found a best feasible solution in the given design constraints.

1 Introduction

Automated design process is attractive for commercial aircraft industry as it greatly reduces a development period by excluding any human interactions. This is very important in today's competitive environment because the commercial success depends on the cost and timeliness of products as well as quality. Toward the automated design of aerodynamic shapes, Computational Fluid Dynamics (CFD) codes have been coupled with various numerical optimization methods.

The gradient-based method (GM) is a well-known optimization algorithm. It probes the optimum by calculating the local gradient information. This method is superior to other optimization algorithms in the local search, while the optimum obtained from this method may not be a global optimum, unless the distribution of the objective is differentiable and convex.

However, distributions of objective functions in real-world applications may be too complex for GM to find an optimum. It is also very difficult for GM to treat realistic constraints. Furthermore, computational time for GM becomes larger as the number of design variables increases, and thus it needs more computational time. For these reasons, GM is not good enough for practical optimizations.

Genetic Algorithm (GA) is an emergent optimization algorithm, which has recently been applied to aerodynamic design problems [1-3]. GA is modeled on the mechanism of the natural evolution. The main idea is the evolution of a population that consists of solution candidates by using selection, crossover and mutation. GA has the capability of finding a global optimum because GA does not use any derivative information unlike GM. In addition, CPU time required for the optimization will not become large as the number of design variables increases. Thus, GA is desirable for practical optimizations.

---

[1] Graduate Student, Department of Aeronautics and Space Engineering.

[2] Associate Professor, Department of Aeronautics and Space Engineering, Senior Member AIAA.

Email: obayashi@ad.mech.tohoku.ac.jp

[3] Professor, Department of Aeronautics and Space Engineering, Associate Fellow AIAA.

[4] Senior Scientist, Computational Sciences Division.

The numerical aerodynamic optimization requires estimation of aerodynamic performance using CFD codes. Among these codes, the Navier-Stokes code is desirable since it evaluates viscous and compressible effect accurately. However, the N-S calculation is very time consuming. Thus, the global optimization coupling GA with the N-S calculations requires incredibly large CPU time even on the latest supercomputers. Previous investigations have therefore been limited to the two-dimensional problems, unless the flow physics was greatly simplified.

In [4], a subsonic wing optimization by GA with three-dimensional N-S calculations was first performed successfully by combining the following features: convergence acceleration by the Multigrid method, simplified airfoil definition, and parallel computation on Numerical Wind Tunnel (NWT, used by winners of IEEE's 1995 and 1996 Gordon Bell Prize for performance). A structural constraint was also applied to obtain a realistic thickness distribution that sustains the bending moment due to the lift generated by the designed wing itself [5]. The resultant design was consistent with the design principles obtained from existing theories and experiments.

In this paper, aerodynamic shape optimizations of a transonic wing with and without the structural constraint are performed by using the simplified airfoil definition as well as the extended Joukowski transformation. For the simplified cases, NACA five-digit airfoil definition is used and only thickness and twist angle distributions are designed. For the extended Joukowski case, the airfoil shape is also optimized by five parameters that define the two consecutive mappings in the complex plane. Similar to [4], aerodynamic performance of each wing design will be evaluated in parallel by using NWT.

2 Transonic wing optimization using NACA airfoil definition

The objective of the present optimizations of a three-dimensional transonic wing is to design a wing geometry that maximizes a Lift-to-Drag ratio (L/D) while maintaining enough wing thickness to stand the bending moment due to the lift distribution. Followings are the detail of the present approach.

2.1 Geometry representation

To model the essence of the design of a wing, spanwise distributions of maximum airfoil thickness and twist angle are selected as design variables. To represent the wing geometry, airfoil shapes are first specified at several spanwise sections using NACA five-digit airfoil series. The airfoil shape is given by NACA230xx where xx is a two-digit number indicating the maximum airfoil thickness to chord in percent. The camber line is specified by the first three digits 230. By using this NACA airfoil definition, the specification of the airfoil shape is reduced to only one parameter. Planform of the wing is assumed to be given by a supercritical wing from the NASA Energy Efficient Transport (EET) Program [6].

Spanwise distributions of thickness and twist angle were described by Spline polygons (control points) of (y, t) and (y, α) where y, t and α are the spanwise location, thickness and twist angle, respectively. Eight polygons are used to determine each distribution, including the fixed wing root and tip locations. The parameter for the thickness is given by a real number between 5 and 20 here. The twist angle is given in degree between -5 and 10. To avoid wavy surface definition, the thickness and twist angle parameters are always rearranged into numerical order from tip to root. The wing surface is interpolated by using the second-order Spline interpolation. Thus, in total, 28 parameters determine the wing design.

2.2 GA operators

In GA, design variables are coded in a finite-length string as genotype. The real number coding is used in this paper. In the real number coding, the length of the string that represents design candidates corresponds to the number of design variables. These strings make up a population to be evolved by GA. Initial population is created randomly.

The evolution process of GA is composed of four operators: evaluation, selection, crossover, and mutation [7]. Figure 1 illustrates the flowchart of GA. Evaluation operator assigns a fitness value to each member of the population according to its objective function value. Here, the fitness value is determined by the ranking of each individual among the population. The objective function is L/D with a penalty for a structural constraint in this study. A Navier-Stokes solver is used to evaluate L/D of each member (design candidate). The flow solver uses TVD type upwind differencing scheme [8] and the LU-SGS implicit scheme [9]. Multigrid method [10] is applied to the N-S code to accelerate the convergence. Evaluation of each member is distributed to one processing element of NWT so that the evaluations are processed in

parallel.

A structural constraint is also introduced to obtain a realistic wing in the transonic regime. For the brevity, the wing and its spanwise lift distribution are replaced by a cantilever and concentrated loads, respectively. From the loads, the bending moment distribution is calculated, which gives the structural stress on the wing. Then the constraint is given so that the local stress is less than the ultimate shear stress of Aluminum alloy 2024-T351 [5].

Selection is a process in which individual strings are copied in mating pool according to their fitness function values. This implies that a string with a higher value has a higher probability of contributing one or more offsprings in the next generation. The stochastic universal sampling [11], instead of the typical roulette-wheel method [7] is used as a selection operator. The best and the second best individuals in each generation are transferred into a new generation without crossover or mutation [12].

In this study, two different crossover operators are used to generate one half of the next generation each: the uniform crossover [13] and the evolutionary direction operator [14]. In the uniform crossover, each pair of strings undergoes exchanges of their genes (design variables); this results in a pair of strings of the new generation. The probability of exchanging each gene is set to 40 %. This crossover contributes to the global search of GA.

The evolutionary direction operator is a modified crossover operator that estimates the direction of evolution from the selected parents. Conventional GA is good at finding a neighborhood of a global optimum but poor at locating an exact optimum within this neighborhood. In other words, convergence of GA becomes slower as it approaches to the optimum. The evolutionary direction operator improves the convergence without any extra CPU time. See [14] for details.

Mutation is a random walk of a string that will occur during the crossover process at a given mutation rate. This operator keeps diversity of a population and promotes the search in the solution space that cannot be represented by the strings of the present population. The combination of mutation and recombination allows in principle for leaving a smaller hill and therefore prevents evolution from getting stuck on local extreme. In this paper, mutation takes place at a probability of 10% and then adds a random disturbance to the parameter in the amount up to ± 1 for the thickness t and the twist angle α, and ± 0.3 for the spanwise location y.

2.3 Results

2.3.1 Aerodynamic design optimization

Transonic wing optimization without the structural constraint was first performed. Aerodynamic optimization was performed at the freestream Mach number of 0.76, an angle of attack of 0 degree and the Reynolds number based on the root chord of 10^7.

The optimization history is illustrated in Figure 2. The entire population converges to an optimum wing in 15 generations. It takes about 80 minutes of CPU time on NWT to advance a generation. The average fitness curve is very close to the best fitness of the population. This is probably because the thickness reached the lower limit of five percent to the chord as shown later. The planform of the designed wing and its airfoil profiles at selected spanwise sections are illustrated in Figure 3.

Wing thickness distribution is shown in Figure 4. Since the thickness of 0.05 chord is the minimum limit of the search space, the wing minimizes the wing thickness as much as possible except at the root region, so as to reduce the wave drag. Wings designed by inverse methods were reported to have disproportionately large thickness near the root similar to the wing designed here.

Figure 5 shows the twist angle distribution of the designed wing in degree. Aerodynamic washout is seen to minimize the induced drag. A twist of more than five degrees is known to result in unacceptably large induced drag increments by experiment [15]. The present design satisfies this design criterion.

Figure 6 shows the resulting lift distribution compared with the parabolic distribution which is known to give the minimum induced drag when the structural constraint is considered [16]. Although no structural constraint is applied here, the lift generated at the outboard section of the wing is suppressed to avoid the excessive wave drag due to the shock wave. This is similar to the lift distribution constraint by the bending moment. Therefore, the computed lift distribution closely resembles the parabola. This figure indicates that the designed wing achieves the minimum induced drag.

Figure 7 shows surface pressure contours on the upper surface. A weak shock wave is seen near the leading edge outboard from the kink location. No flow separation was found. The straight isobar pattern suggests that the flow field is nearly two dimensional in the spanwise direction. It indicates a good design since it gives the same drag-divergence Mach number from root to tip. From these observations, GA has found an optimum solution in the design space.

2.3.2 Effect of structural constraint

Next, the structural constraint is applied to the aerodynamic optimization. The convergence history of the present optimization is shown in Figure 8. The optimum was obtained in 50 generations. During the optimization, some members had a strong shock wave or failed to satisfy the structural constraint. However they were weeded out from the population because of the resultant penalties to the fitness. Wing geometry of the designed wing is presented in Figure 9.

Wing thickness distribution is given in Figure 10. The maximum thickness constraint appears at the kink and the designed thickness distribution satisfies it. At the wing tip the thickness is 0.05, that is, the minimum thickness in the search space. The designed wing is the thinnest wing allowed by the structural constraint. Figure 11 illustrates the twist angle distribution.

Figure 12 compares the computed spanwise load distribution with the parabolic loading distribution. The optimized wing has failed to realize the parabolic distribution. The lift at the midspan region is required to be increased to achieve the parabolic distribution, but it would result in an unacceptably large wave drag associated with a stronger shock wave.

Pressure contours in Figure 13 illustrate the flow structure on the upper surface of the designed wing. The pressure contours are nearly two-dimensional in the spanwise direction, despite of the large variation of thickness and twist angle distributions. No flow separation was seen, although a strong shock wave was found at the midspan.

These results indicate that there is a tradeoff between the increase of the structural strength and the reduction of the wave drag. With the present simplified airfoil definition, the wing thickness enough to stand the bending moment causes a strong shock wave since NACA 5-digit series are subsonic airfoils. Nevertheless, GA has found a best feasible solution under the structural constraint.

Breakthrough for the dilemma of having enough thickness and avoiding a strong shock wave has been given by supercritical airfoil sections. This leads to a wing optimization with the airfoil shape optimization at each section. However, such an approach will require much more control points, which lead to an order of magnitude increase of the design variables. Hence a proper encoding method with smaller design variables is desired. As a candidate for this, the extended Joukowski airfoil definition is considered in the next section.

3 Transonic wing optimization using the extended Joukowski transformation

3.1 Geometry representation

In this section, airfoils are represented by the extended Joukowski transformation. It transforms a unit circle to various kinds of airfoils in the complex number plane by two consecutive conformal mappings as,

$$Z_0 = re^{i\theta} + Z_c \tag{1}$$

$$Z_1 = Z_0 - \varepsilon / (Z_0 - \Delta) \tag{2}$$

$$Z = Z_1 + 1 / Z_1 \tag{3}$$

here Z_c, Z_0, Z_1, Z, and ε are complex numbers and Δ, r, and θ are real numbers.

This transformation is therefore defined by Z_c, ε, and Δ where r is determined so that Z_0 passes the origin of the coordinate axes. In this study, a position (x_c,y_c) which is the center of the unit circle Z_0, a position (x_t,y_t) which is transformed to the trailing edge of the resulting airfoil, and the preliminary movement in the real axis Δ are used as the design variables, because x_c, x_t, and Δ are known to contribute to the airfoil thickness while y_c and y_t define the airfoil camber line. The complex number ε is given by (x_t,y_t). As a result, an airfoil shape is specified by five parameters.

Spanwise distributions of the extended Joukowski parameters and twist angle are then described by Spline polygons (control points) of (y_j,J_i) i=1,…,5 and (y_α,α) where y, J_i and α are the spanwise location, the extended Joukowski parameters and twist angle, respectively. These

design variables are bounded as Table 1:

Design Variable	Lower-bound	Upper-bound
$J_1(x_c)$	-0.1	0
$J_2(y_c)$	0	0.1
$J_3(x_t)$	1	1.05
$J_4(y_t)$	-0.05	0.05
$J_5(\Delta)$	0	0.8
y_J	0	1.88
α	-5 deg.	10 deg.
Y_α	0	1.88

Table 1 Boundaries of design variables
(root chord = 1)

Five polygons are used to determine each distribution, including the fixed polygons at the wing root and tip. The extended Joukowski parameters are again rearranged from tip to root according to the airfoil thickness so that the resulting wings always have maximum thickness at the wing root. The twist angle parameter is also rearranged into numerical order from tip to root. The wing surface is interpolated by using the second-order Spline interpolation. In total, 34 parameters determine a wing geometry.

When the initial population is created randomly, most of the population do not satisfy the constraint. Thus, GA converges prematurely. To avoid this, the initial population is created as follows. 1) The preliminary population is created randomly in the design space. 2) The population is evolved to obtain 10 design candidates that satisfy the structural constraint. 3) The initial population is created by these 10 individuals and their mutants. Mutants are made from a random disturbance to the extended Joukowski parameters in the amount up $\pm$10% of the range given in Table 1.

3.2 Results

The final optimization was performed at the freestream Mach number of 0.8, an angle of attack of 0 degree and the Reynolds number based on the root chord of 10^7. The freestream Mach number is higher than that of the previous case by 0.04. The population size is reduced to 50. Figure 14 illustrates the convergence history. The resultant wing has the rear loading, as thus the lift-to-drag ratio has increased to 19.56.

Figure 15 shows surface pressure contours on the upper surface of the designed wing. Compared to Figure 13, the shock wave is weakened and only seen between the two kink locations, although the isobar pattern is lost. Figure 16 illustrates the spanwise lift distribution. The parabolic distribution was not achieved, either. This is probably due to a premature convergence as seen in the thickness distribution of the designed wing in Figure 17. The plot indicates that the wing is unnecessarily thick.

To obtain an optimum thickness, three of the extended Joukowski parameters have to cooperate with each other. There is a possibility, though, that crossover operator destroys their cooperation. Further investigations are necessary for appropriate GA operators as well as the airfoil definition.

4 Conclusions

GA has been applied to optimize a transonic wing shape for generic transport aircraft by using the three-dimensional compressive Navier-Stokes equations with a structural constraint on the wing thickness. To overcome enormous computational time necessary for this optimization the N-S computations were processed in parallel on NWT. As a result, the CPU time for one generation was reduced to about 80 minutes on NWT, and thus the total CPU time necessary for the optimization became about 2 days.

The transonic wing optimization using NACA airfoil definition were first performed without the structural constraint. The designed wing has a fully attached flow and the allowable minimum thickness so that profile drag and wave drag are minimized. The resulting parabolic loading indicates that the induced drag is also minimized in this problem. These results confirm the validity of the present approach.

In the next optimization case with the structural constraint, a tradeoff between the increase of the structural strength and the reduction of the wave drag was observed. The multidisciplinary optimization approach considering both structural and aerodynamic optimization will be investigated in future.

In the final optimization case, the extended Joukowski transformation was used for the airfoil definition of the wing. Though L/D was improved even at a higher Mach number

than the previous cases, only a premature solution was obtained. To obtain a fully converged optimum design, further investigations should be made into the GA operators such as initialization of a population and crossover. In addition, an appropriate airfoil definition will be examined by using the multiple mappings in the Joukowski transormation.

Acknowledgement

This work was partly supported by de Havilland Inc., Canada.

REFERENCES

[1] Gage, P. and Kroo, I., "A Role for Genetic Algorithms in a Preliminary Design Environment," AIAA Paper 93-3933, 1993.

[2] Obayashi, S. and Tsukahara, T., "Comparison of Optimization Algorithms for Aerodynamic Shape Design," AIAA Paper 96-2394, 1996.

[3] Yamamoto, K. and Inoue, O., "Applications of Genetic Algorithm to Aerodynamic Shape Optimization," AIAA Paper 95-1650, 1995.

[4] Obayashi S. and Oyama, A., "Three-Dimensional Aerodynamic Optimization with Genetic Algorithm," the Second ECCOMAS Conference on Computational Fluid Dynamics, Paris, September, 1996.

[5] Case, J., Chilver, A. H., and Ross, C. T. F., *Strength of Materials & Structures with an Introduction to Finite Element Methods*, 3rd Edn., Edward Arnold, London, 1993.

[6] Jacobs, P. F., "Experimental Trim Drag Values and Flow-Field Measurements or a Wide-Body Transport Model with Conventional and Supercritical Wings," NASA TP 2071, 1982.

[7] Goldberg, D. E., *Genetic Algorithms in Search, Optimization and Machine Learning*, Addison-Wesley Publishing Company, Inc., Reading, 1989.

[8] Obayashi, S. and Wada, Y., "Practical Formulation of a Positively Conservative Scheme," *AIAA Journal*, 32, 1093-1095, 1994.

[9] Yoon, S., Jameson, A. and Kwak, D., "Effect of Artificial Diffusion Scheme on Multigrid Convergence," AIAA Paper 95-1670, 1995.

[10] Jameson, A., "Solution of the Euler Equations for Two-Dimensional Transonic Flow by a Multigrid Method," *Applied Mathematics and Computation*, Vol.13, pp. 327-356, Nov. 1983.

[11] Baker, J. E., "Reducing Bias and Inefficiency in the Section Algorithm," Proceedings of 2nd International Conference on Genetic Algorithm, 1987.

[12] Davis, L., *Handbook of Genetic Algorithms*, Van Nostrand Reinhold, New York, 1990.

[13] Michalewicz, Z. and Schoenauer, M., "Evolutionary Algorithms for Constrained Parameter Optimization Problems," *Evolutionary Computation*, Vol. 4, No. 1, pp. 1-32, 1996.

[14] Yamamoto, K. and Inoue, O., "New Evolutionary Direction Operator for Genetic Algorithm," *AIAA Journal*, Vol. 33, No. 10, pp. 1990-1992, Oct. 1995.

[15] Torenbeek, E., *Synthesis of Subsonic Airplane Design*, Kluwer Academic Publishers, Dordrecht, 1982.

[16] Jones, R.T., *Wing Theory*, Princeton University Press, 1990.

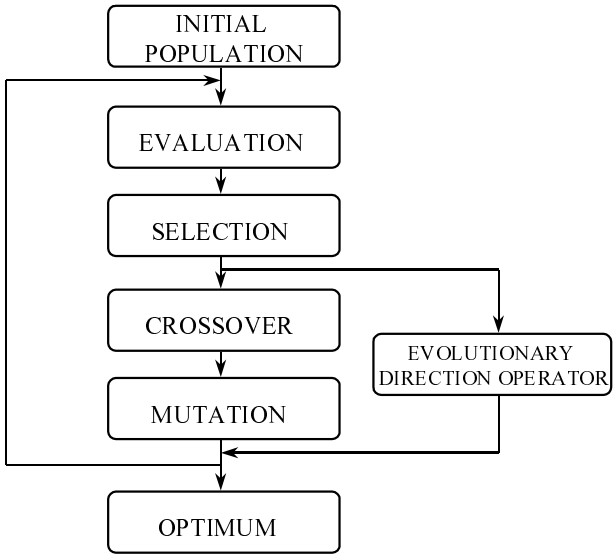

Figure 1 Flowchart of GA

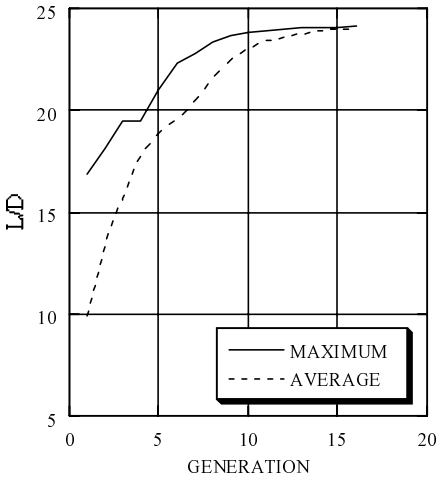

Figure 2 Optimization history

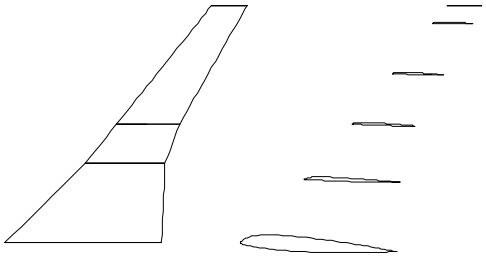

Figure 3 Optimum wing design

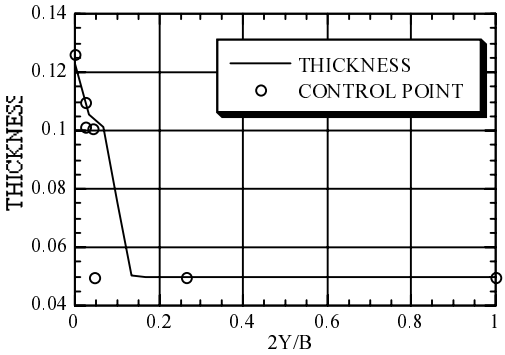

Figure 4 Spanwise thickness distribution

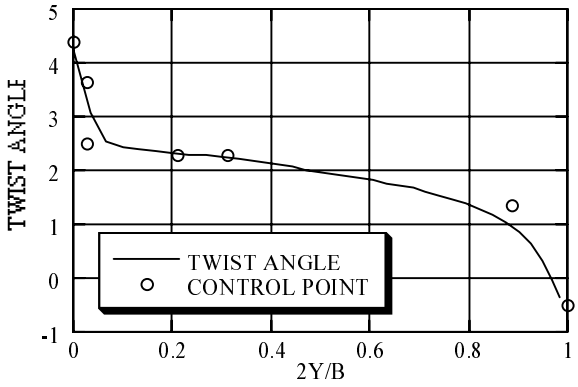

Figure 5 Spanwise twist angle distribution

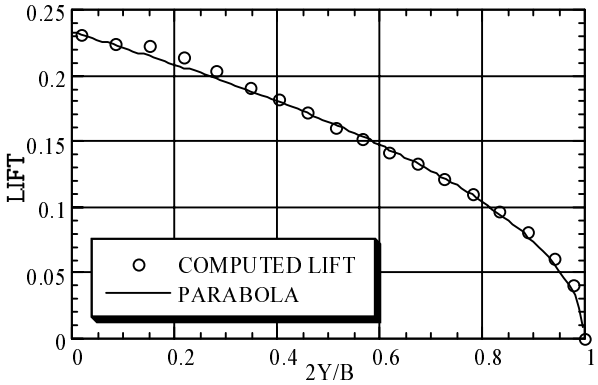

Figure 6 Spanwise lift distribution

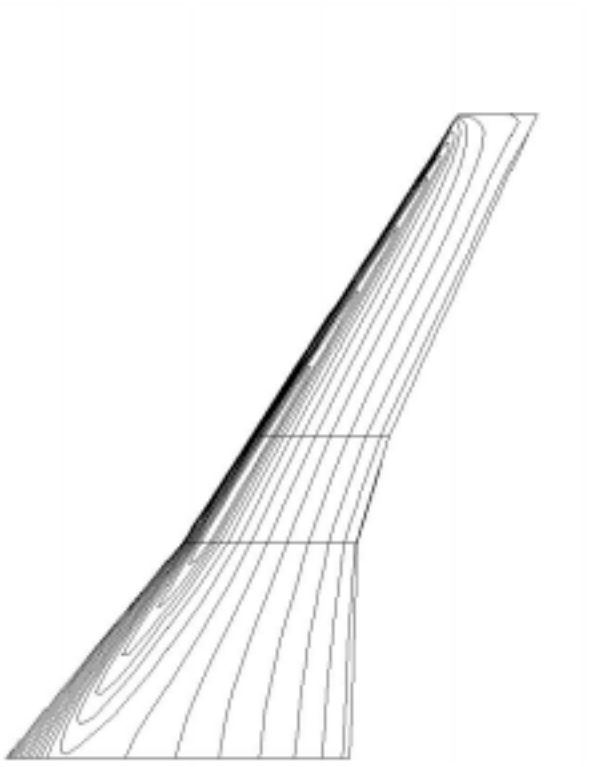

Figure 7 Pressure contours on the upper surface

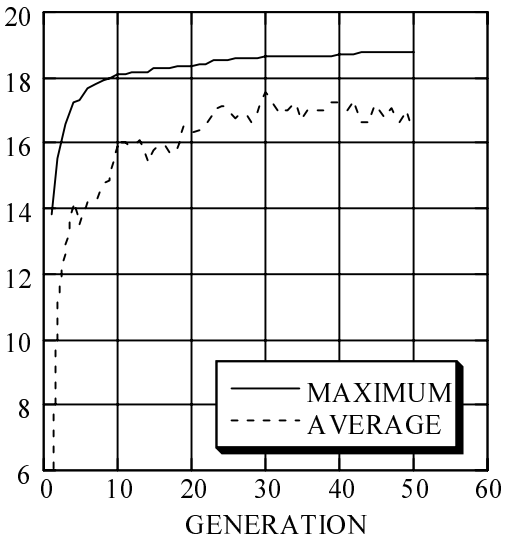

Figure 8 Optimization history

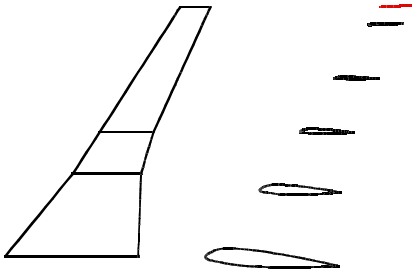

Figure 9 Optimum wing design

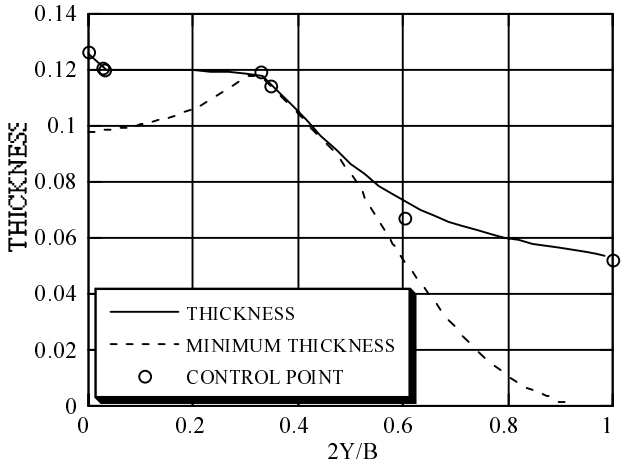

Figure 10 Spanwise thickness distribution

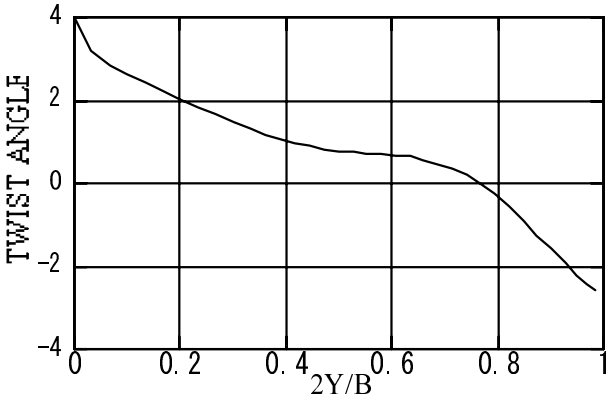

Figure 11 Spanwise twist angle distribution

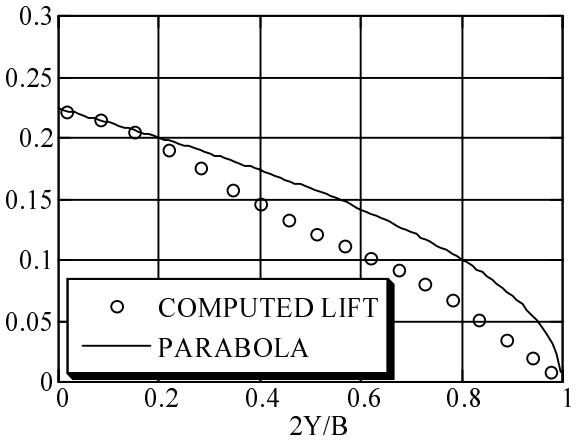

Figure 12 Spanwise lift distribution

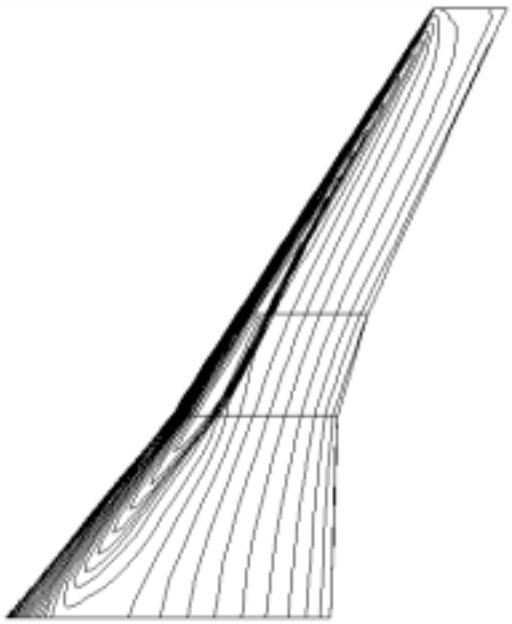

Figure 13 Pressure contours on the upper surface

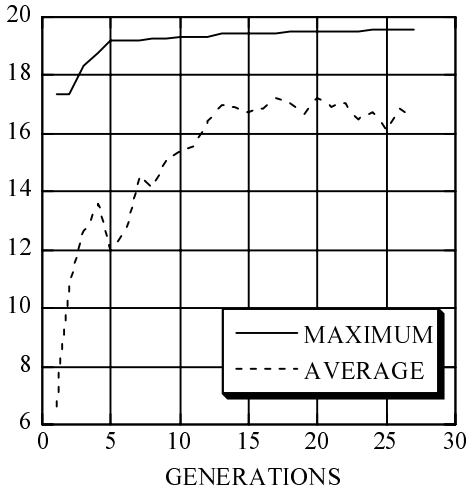

Figure 14 Optimization history

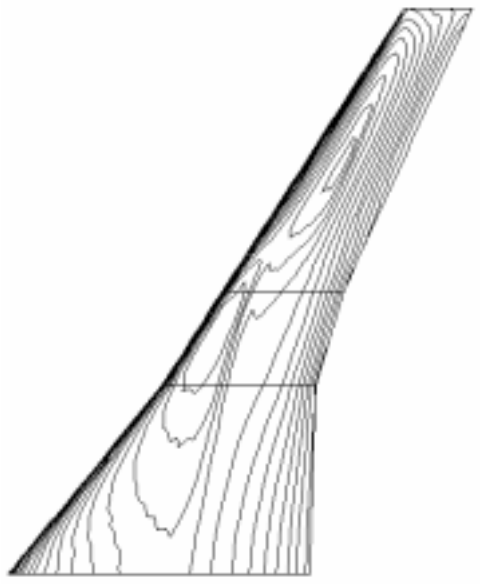

Figure 15 Pressure contours on the upper surface

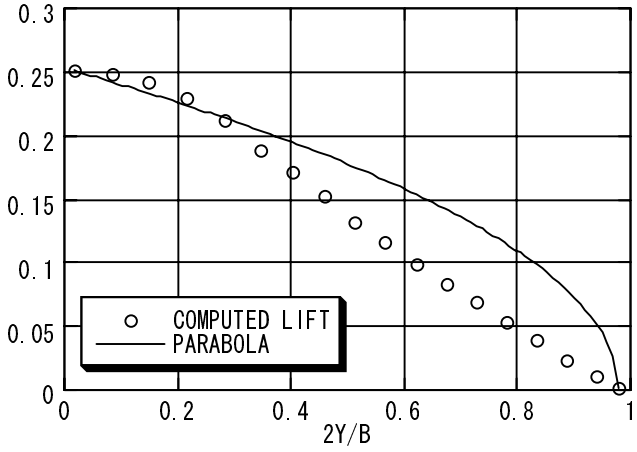

Figure 16 Spanwise lift distribution

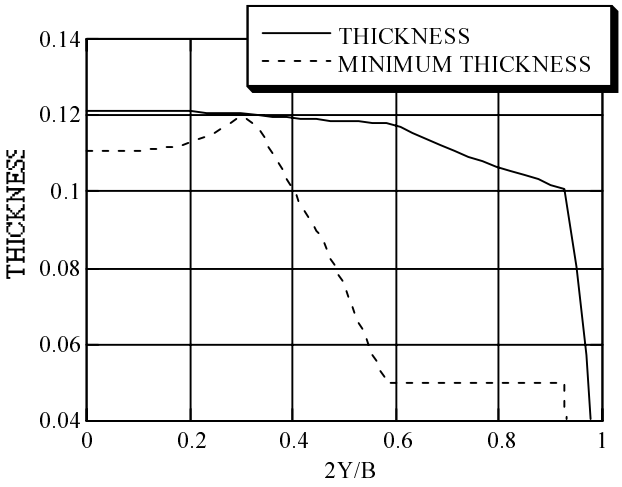

Figure 17 Spanwise thickness distribution